Pure appl. geophys. 162 (2005) 1643–1672
0033 – 4553/05/091643–30
DOI 10.1007/s00024-005-2687-6

Pure and Applied Geophysics

Air-sea Coupling During the Tropical Cyclones in the Indian Ocean: A Case Study Using Satellite Observations

BULUSU SUBRAHMANYAM,[1] V.S.N. MURTY,[2] RYAN. J. SHARP,[1] and JAMES. J. O'BRIEN[1]

Abstract—In the years 1999 and 2001, three intense tropical cyclones formed over the northern Indian Ocean—two over the Bay of Bengal during 15–19 and 25–29 October, 1999 and one over the Arabian Sea during 21–28 May, 2001. We examined the thermal, salinity and circulation responses at the sea surface due to these severe cyclones in order to understand the air-sea coupling using data from satellite measurements and model simulations. It is found that the Sea Surface Temperature (SST) cooled by about 0.5 °–0.8 °C in the Bay of Bengal and 2 °C in the Arabian Sea. In the Bay of Bengal, this cooling took place beneath the cyclone center whereas in the Arabian Sea, the cooling occurred behind the cyclone only a few days later. This contrasting oceanic response resulted mainly from the salinity stratification in the Bay of Bengal and thermal stratification in the Arabian Sea and the associated mixing processes. In particular, the cyclones moved over the region of low salinity and smaller mixed layer depth with a distinct mixed layer deepening to the left side of the cyclone track. It is envisaged that daily satellite estimates of SST and Sea Surface Salinity (SSS) using Outgoing Longwave Radiation (OLR) and model simulated mixed layer depth would be useful for the study of tropical cyclones and prediction of their path over the northern Indian Ocean.

Key words: Tropical cyclones, Indian Ocean, EOL, OLR, sea-surface salinity, mixed layer depth, Remote Sensing.

1. Introduction

Tropical cyclones, the intense swirling motions of air moving cyclonically around a low-pressure center in the Northern Hemisphere and influencing vast horizontal distances in space, form over warmer oceanic regions where the Sea Surface Temperature (SST) is above 26 °C. In the tropical Indian Ocean, cyclones form over both the Bay of Bengal and the Arabian Sea and there are marked seasonal variations in their places of origin, tracks and intensities (ANONYMOUS, 1979). The

[1]Center for Ocean-Atmospheric Prediction Studies, The Florida State University, Tallahassee, FL 32306-2840, U.S.A.
[2]Physical Oceanography Division, National Institute of Oceanography, Goa, 403 004, India.

life span of a severe cyclonic storm over the Indian Ocean averages about 4 days from the time it forms until the time it makes landfall. On a yearly basis, the number of cyclones over the Bay of Bengal is 3–4 times more those over the Arabian Sea (ANONYMOUS, 1979; OBASI, 1997). Over the Bay of Bengal, tropical cyclones form during April-May over the southern and central Bay and move initially northwest striking the Indian coast and at times change gradually to a northward direction towards Bangladesh and at times recurve towards the Mynamar coast. Severe intensity tropical cyclones form during October-November mostly over the southern and central Bay and Andaman Sea and move westward towards the east coast of India and sometimes recurve between 15 ° and 18 °N affecting the Bangladesh coast. Weakened Pacific typhoons rejuvenate into low-pressure systems over the Andaman Sea and intensify further over the Bay during October-November. These cyclones give rise to copious rainfall and often cause major inland flooding and associated damage and loss of life in the eastern portion of the Indian subcontinent. In the Arabian Sea, cyclones generally form over southeast and central regions in May, October through December and in east central Arabian Sea in June. Some of the cyclones that originate in the Bay of Bengal travel across the peninsula, weaken and emerge into the Arabian Sea as low-pressure systems and may again intensify into cyclonic storms (ANONYMOUS, 1979). Knowledge of the ocean response to storm forcing is one of the key factors in tropical cyclone track prediction. Monitoring of surface weather parameters and the upper ocean thermal structure from moored buoys has become a key element in the studies of tropical cyclones and the ocean's response (PREMKUMAR *et al.*, 2000). Many studies were carried out to document the ocean's response to the tropical cyclones and to understand the associated air-sea interaction processes (for example, STRAMMA *et al.*, 1986; SHAY, 1994; SHAY *et al.*, 2000; GINIS, 2002). Tropical cyclones are driven by turbulent heat fluxes from the ocean and induce rapid changes in the heat and buoyancy fluxes and the currents in the oceanic mixed layer over a very short span of time (few days to weeks) and the magnitude of such processes are known only to some extent, particularly for the western Atlantic and Pacific. Because of this, one can conclude that the response of the upper ocean to the passing storm plays a major role in controlling the storm intensity through associated variability in the upper ocean conditions (such as surface temperature, surface salinity, mixed layer depth, currents in the mixed layer, etc.) and atmospheric conditions (such as winds, atmospheric pressure, and rainfall/precipitation). In the case of the tropical Indian Ocean, earlier investigators (RAO, 1987; GOPALAKRISHNA *et al.*, 1993; MURTY, 1983; MURTY, *et al.*, 1996; SEETARAMAYYA *et al.*, 2001; CHINTHALU *et al.*, 2001) reported cooling of the sea-surface temperature (SST) due to the passage of cyclones in the Bay of Bengal and Arabian Sea. They noted that in regions of weaker upper ocean stratification (southern and western Bay of Bengal), magnitude of the SST decreases due to the cyclone was around 2 °C (RAO, 1987; GOPALAKRISHNA *et al.*, 1993) while in the northern Bay where the upper ocean stratification is strong due to low salinity

waters, the SST decrease was between 0.3 °C and 0.9 °C (MURTY *et al.*, 1996; SEETARAMAYYA *et al.*, 2001; VINAYCHANDRAN *et al.*, 2002). This cyclone-induced SST decrease appears to lead to horizontal temperature gradients and in turn the pressure gradients in the atmosphere, thereby further affecting the intensity of the cyclone. However, the above studies have not indicated the variation of sea-surface salinity (SSS) during the storm period, as there was a lack of observations. During the Typhoon 90 Experiment in the western Pacific, the extensive observations indicated a significant decrease of SSS in the regions directly influenced by precipitation (SHAY, 1994).

Figures 1a–b show the paths of two tropical cyclones (TC) 04B and 05B that developed over the Bay of Bengal during 15–19 October and 25–30 October, 1999. TC 04B reached maximum intensity on October 17, 1999 before making landfall at the east coast of India. TC 05B was designated as a ''Super Cyclone,'' it was the most

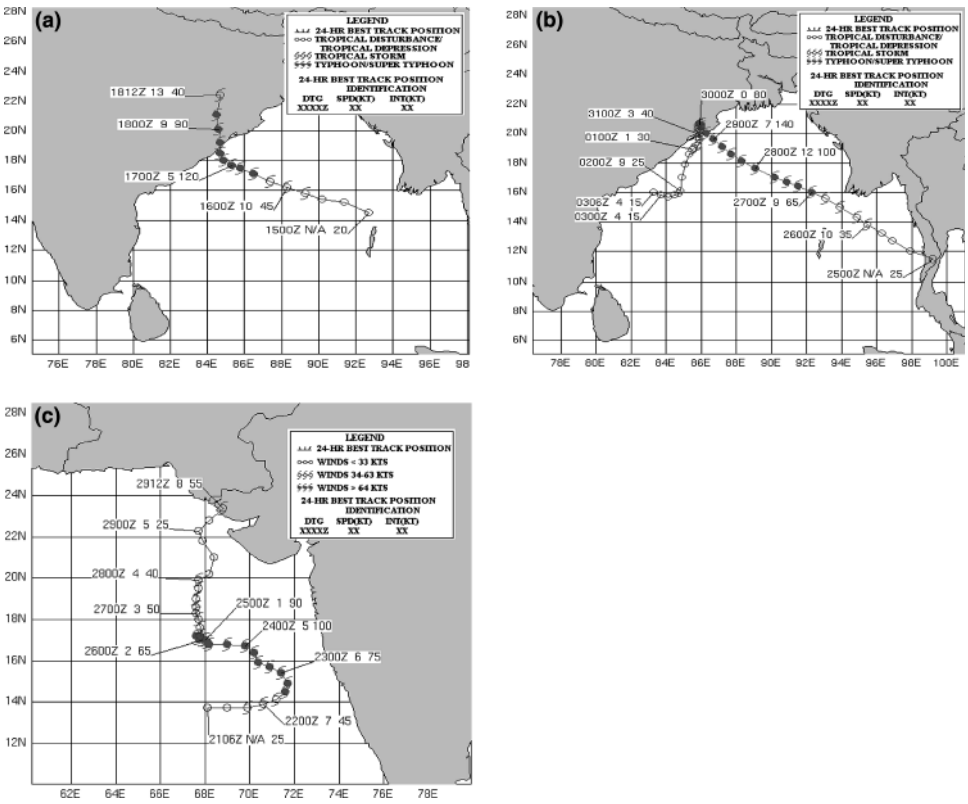

Figure 1
Tracks of tropical cyclones during (a) October 15–19, 1999 (TC 04B), (b) October 25–29, 1999 (TC 05B) in the Bay of Bengal and (c) May 21–28, 2001 (TC 01A) in the Arabian Sea (obtained from Joint Typhoon Warning Center, USA).

powerful tropical cyclone on record to affect coastal India. TC 05B developed from a disturbance that originated in the South China Sea and tracked through the Gulf of Thailand and across the Malay peninsula before strengthening over the Andaman Sea. It intensified at a greater rate than the climatological rate, peaking on October 28 at 1800Z as a Very Severe Cyclonic Storm (VSCS) and made landfall after 11 hours. LAL (2001) in his review on tropical cyclones had listed both TC 04B and 05B and discussed their consequences. Figure 1c shows the path of the first tropical cyclone in the year 2001 (TC 01A) which formed and developed over the eastern Arabian Sea during May 21–28. As the system intensified, it moved in a northwesterly direction and as it weakened, it moved in a northerly direction.

In this study, we describe the air-sea coupling through the ocean's thermal, salinity and circulation responses at sea surface due to these intense tropical cyclones in the northern Indian Ocean with a new observational method, based on satellite measurements and mixed layer model simulations.

2. Data and Methods

Wind stress derived from SeaWinds on QuikSCAT scatterometer was differentiated to derive the vorticity fields during the periods of tropical cyclones 04B (15–19 October, 1999), 05B (25–30 October, 1999) and 01A (21–28 May, 2001). SHARP *et al.* (2002) showed that vorticity could be used as a tool to identify areas of tropical cyclogenesis. Vorticity was calculated within the SeaWinds swath rather than from a regularly gridded product to obtain high resolution within the swath. SeaWinds data are freely available via the web http://www.coaps.fsu.edu from the Center for Ocean-Atmospheric Prediction Studies (COAPS) at Florida State University, U.S.A. Surface pressures were objectively calculated for the periods of tropical cyclones 04B, 05B and 01A using the method by HILBURN *et al.* (2003).

Daily OLR data on $2.5\,^{\circ} \times 2.5\,^{\circ}$ grids were obtained for the periods of cyclones (October 1999 and May 2001) from Climate Diagnostics Center (CDC), Boulder, Colorado, U.S.A. MURTY *et al.* (2000, 2002, 2003) reported that intense convection over the tropical Indian Ocean is closely coupled to the oceanic surface layer conditions (temperature and salinity) through the oceanic parameter, the Effective Oceanic Layer (EOL) which is linearly related to the OLR. The EOL is defined as the geopotential thickness (m^2/s^2) of the near-surface stratified layer, chosen as 30 m thick from sea-surface. This means that the EOL represents the sea-surface elevation in dynamic centimeters (dyn.cm) relative to the 30 db level. Climatological monthly temperature and salinity data from the World Ocean Atlas (WOA98; ANTONOV *et al.*, 1998 and BOYER *et al.*, 1998) were used to compute the monthly EOL. Regression relationships (algorithms) were then obtained between the EOL and the WOA98 SST for each month and the algorithms for October and May are mentioned in Sections 3.4 and 3.5. The 16 year-mean monthly OLR data and the

computed monthly EOL data were used to develop relationships between OLR and EOL for each month for the Bay of Bengal and the Arabian Sea (MURTY *et al.*, 2004). Similarly, algorithms were also obtained between the 16 year-mean monthly OLR and monthly WOA98 SSS for each month (MURTY *et al.*, 2004). These monthly algorithms (OLR-EOL-SST and OLR-SSS) are applied to the synoptic data for the periods of the cyclones. Mention is made here that we noticed an improvement in the correlation coefficients for the OLR-EOL and OLR-SSS relationships for October, when compared to that reported in MURTY *et al.* (2002). This is attributed to the additional OLR data and the improved WOA98 climatology from that of LEVITUS *et al.* (1994a,b) climatology. The daily OLR values over the Bay of Bengal and Arabian Sea during the periods of cyclones were far lower than the respective 16 year-mean monthly OLR. Therefore, in order to estimate the SSS, a 2^{nd} degree polynomial relationship between the 16 year-mean OLR and WOA98 SSS (specific for this study) was used for October only for the Bay of Bengal and a linear relationship for May for the Arabian Sea (as proposed by MURTY *et al.*, 2004). The U.S. Navy's Modular Ocean Data Analysis System (MODAS) daily SSS data (FOX *et al.*, 2002a,b), provided by Naval Research Laboratory (NRL) at Stennis Space Center, Mississipi, U.S.A., were also examined for the periods of cyclones 04B, 05B and 01A. In addition, daily values of precipitation and SST from the Tropical Rainfall Measuring Mission (TRMM) on $0.25\,^{\circ} \times 0.25\,^{\circ}$ grids were obtained from Remote Sensing Systems (http://www.remss.com/tmi). Finally, the Navy Layered Ocean Model (NLOM) simulated SST and mixed layer depth (MLD) data (KARA *et al.*, 2000, 2003a,b), as provided by Naval Research Laboratory at Stennis Space Center, Mississipi, U.S.A. were also utilized. This NLOM has $1/8\,^{\circ}$ resolution and forced with the six-hourly reanalysis winds obtained from the European Center for Medium-Range Weather Forecasts (ECMWF) Reanalysis; the SST simulation was available on a daily basis while the simulated mixed-layer-depth (MLD) was available as averages of 3.05 days to suppress the effect of inertial oscillations.

3. Results and Discussion

3.1 Surface Wind Field and Sea-level Pressure during the Tropical Cyclones

The cyclone 04B was located at 16.0 °N, 88.5 °E at 0300 Z and at 17.8 °N, 87 °E at 1200 Z on 16 October and moved across the Bay of the Bengal in three days while intensifying into VSCS on 17–18 October (Fig. 1a). This system weakened as Deep Depression (DD) on 19 October over the land. The cyclone 05B system moved in a northwesterly direction across the Bay of Bengal in 5 days from 25 October over the eastern Andaman Sea to 29 October over the northwestern Bay (Fig. 1b). This system also developed into VSCS stage on 28 October and further intensified over

land into a 'Super Cyclone' on 30 October. The Indian Daily Weather Reports (IDWRs) issued by the India Meteorological Department (IMD) reported a central pressure of 996 hpa on 28 October at the VSCS stage.

The SeaWinds-derived voriticity fields and mean sea-level pressures associated with the cyclones 04B and 05B identified the regions with stronger wind speeds (30–35 knots), larger cyclonic (positive) vorticity (and associated convergence) and the rain band structures for each cyclone. On 16 October, the cyclonic vorticity was strong (20–25$\times 10^{-5}$ s^{-1}) at the center of the cyclone (Fig. 2a) and extended over a 2 °$\times$2 ° degree area with its axis oriented in a southwest-northeast direction,

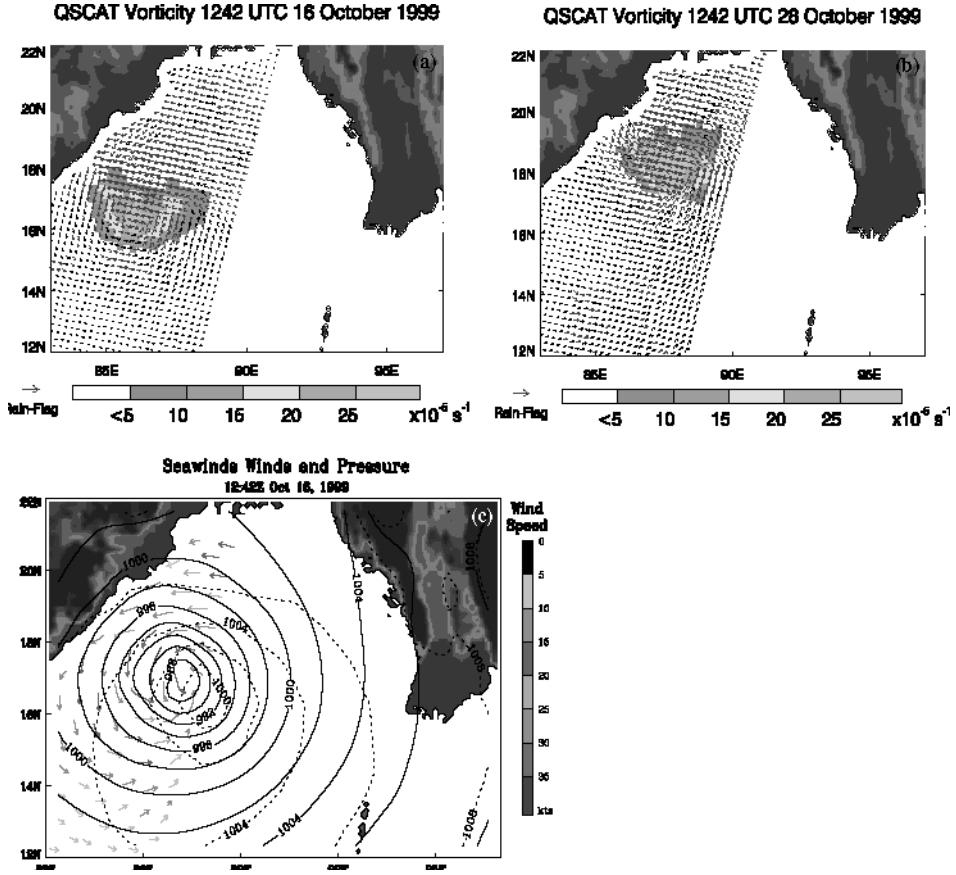

Figure 2
SeaWinds Scatterometer winds derived vorticity fields for (a) October 16, 1999, (b) October 28, 1999 during the intense stages of TC 04B and TC 05B respectively, with red arrows indicating the multi-dimensional histogram (MUDH) flagged rainfall, and (c) SeaWinds calculated mean sea-level pressure (thick black lines), with ECMWF background mean sea-level pressure (black dotted lines) and wind speed color vectors for October 16, 1999 during TC 04B.

identifying the path of the cyclone. The intense positive vorticity field at 1242 UTC (Fig. 2a) weakened towards the north by 2348 UTC on the same day while the rain band intensified in the western sector (figure not shown). The SeaWinds-derived vorticity fields during cyclone 05B was more intense (than that of 04B) reaching a vorticity of $25–30\times10^{-5}$ s^{-1} by 1242 UTC on 28 October (Fig. 2b). The SeaWinds-derived mean sea-level pressure (solid lines) and the ECMWF reanalysis mean sea level pressure (dotted lines) on 16 October (Fig. 2c) showed a difference of 12 hPa at the center of the cyclone. The SeaWinds calculated pressure was 988 hPa whereas the ECMWRF analyzed pressure was 1000 hPa. The IDWRs reported a central pressure of 1002 hPa at the center of the cyclone (CHINTHALU *et al.*, 2001) which was close to the ECMWF pressure at the cyclone center. The isobars were closer in the northwestern sector of the cyclone and wide in its southeastern sector. The isobars of mean sea-level pressure nearly coincided with those reported by the IDWRs (CHINTHALU *et al.*, 2001). The wind vectors showed a converging inward flow of speed up to 30–35 knots at the northwestern sector of the cyclone. The techniques developed by TURK and BANKS (1996) were used to plot the wind vectors superimposed on the surface pressure.

In the Arabian Sea, the SeaWinds-derived vorticity field for cyclone 01A clearly shows its location, intensity, extent and shift (movement) . The cyclone moved 4 ° in latitude from 23 May to 28 May, when it started weakening. The cyclone intensified on 24 May reaching a vorticity of $25–30\times10^{-5}$ s^{-1} at the cyclone center (17.5 °N, 68.5 °E)(Fig. 3a). The rain band was located on the southern edge of the cyclone. The SeaWinds-calculated mean sea-level pressure showed convergence of air towards the center of the cyclone and the central pressure reached as low as 988 hPa on 28 May (Fig. 3b). However, the ECMWF reanalysis mean sea-level pressure at the center of the cyclone was 996 hPa (black dotted contours in Fig. 3b).

3.2 OLR during the Tropical Cyclones

In association with the development of the weather systems 04B and 05B from depression to VSCS/Super cyclone stages, intense deep-convection took place over the Bay of Bengal. The zone of intense convection was identified with the zone of low OLR. The cyclone track was superimposed on the OLR distribution maps and the position of cyclone center at 1200Z on each day was marked (Fig. 4). On 15 October, the center of the 'depression' was characterized with a low OLR of 160 W/m^2 west of the Andaman Islands (Fig. 4a). On subsequent days, the low OLR zone followed the track of the weather system. The low OLR zone shifted to the northwestern Bay when the weather system intensified into the VSCS stage on 17 October (Fig. 4b) and the OLR was relatively high ($\sim$200 W/m^2) in the southeastern sector of the system. The weather system 05B was characterized by low OLR ranging from 120–140 W/m^2 (this low was much lower than that of cyclone 04B) at its center (Fig. 4c) and could be used to track the system during its movement across the Bay. On 28 October, the

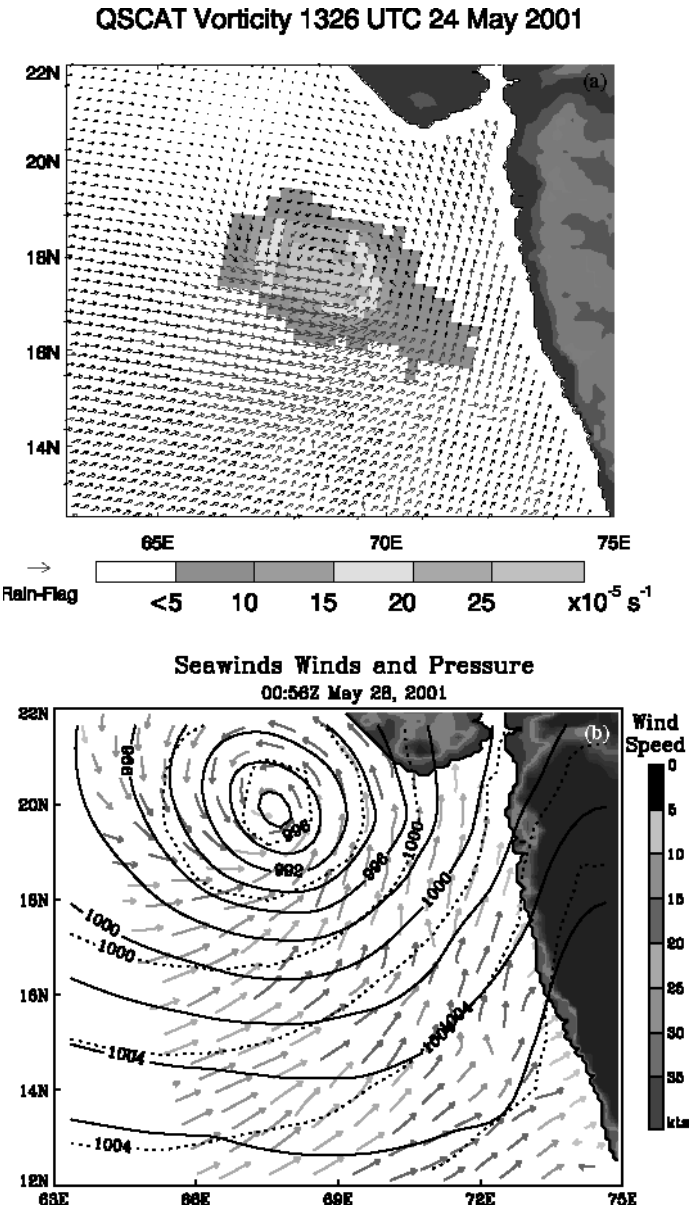

Figure 3

SeaWinds Scatterometer winds derived (a) vorticity field for May 24, 2001 during the intense stage of TC 01A, with red arrows indicating the multi-dimensional histogram (MUDH) flagged rainfall and (b) SeaWinds calculated mean sea-level pressure (thick black lines), with ECMWF background mean sea-level pressure (black dotted lines) and wind speed color vectors for May 28, 2001 during weakening stage of TC 01A.

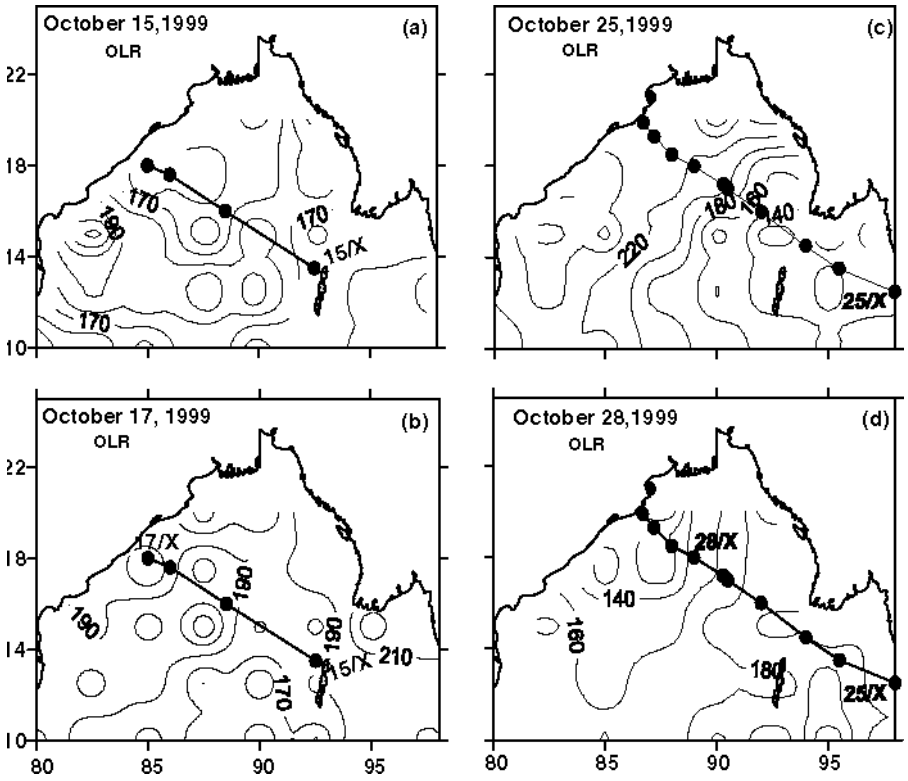

Figure 4
Variation of satellite measured Outgoing Longwave Radiation (OLR) during various stages (initial and intense) of (a–b) TC 04B (left panel) and (c–d) TC 05B (right panel).

system intensified into VSCS stage and the low OLR zone (< 140 W/m^2) shifted to the northwestern Bay (Fig. 4d).

In the Arabian Sea, one would see a change in the pattern of OLR during the TC 01A. Initially, on 21 May the OLR was minimum at 180 W/m^2 before the development of the weather system (Fig. 5a). On the day of its development into depression, i.e., on 24 May, a zone of low OLR (< 140 W/m^2) formed slightly to the left of the cyclone track (Fig. 5b). At the weakening stage of the cyclone on 28 May, the low OLR (< 240 W/m^2) zone shifted westwards while the cyclone moved northward towards the Indian peninsula (Fig. 5c).

3.3 EOL and the Inferred Surface Circulation during the Tropical Cyclones

The linear relation between the 16 year-mean OLR and climatological EOL had a correlation coefficient of $r^2 = 0.36$ in October in the Bay of Bengal (MURTY *et al.*, 2004). MURTY *et al.* (2002) obtained a correlation coefficient of $r^2 = 0.16$ for

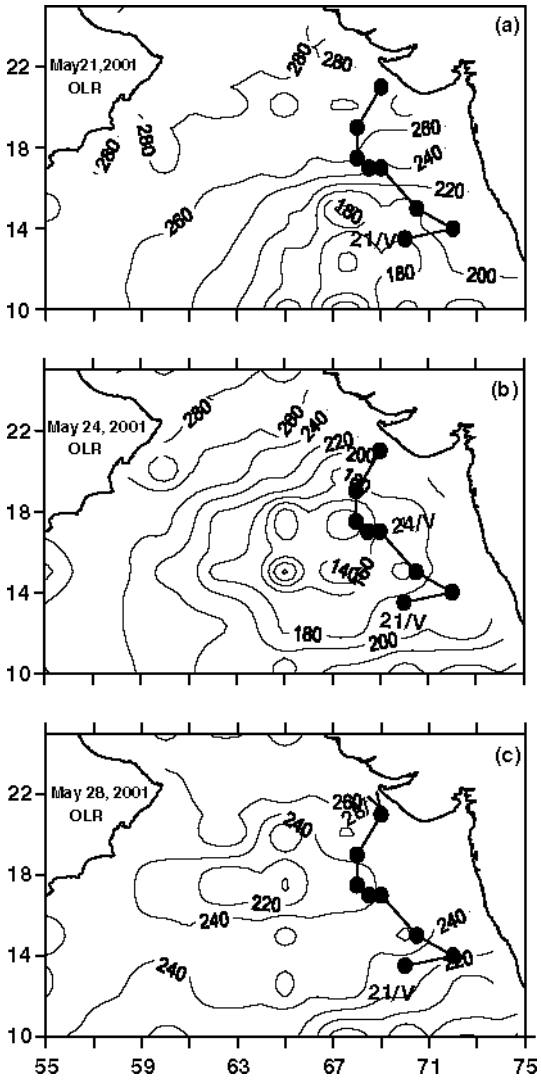

Figure 5
Daily variation of (a–c) satellite measured Outgoing Longwave Radiation (OLR) during various stages (initial, intense and weakening) of TC 01A.

October, with the 13 year-mean INSAT 1-D OLR and the climatology of LEVITUS *et al.* (1994a,b). Using this relationship (EOL = 0.0171*OLR – 1.511, $r^2 = 0.36$), the EOL was estimated (E_{eol}) at each grid point (2.5 °×2.5 °) from the daily OLR during the periods of TC 04B and TC 05B. The variation of E_{eol} facilitates to understanding the near-surface circulation under the influence of weather systems. Cyclonic

(anticyclonic) circulation is inferred around the lower (higher) E_{eol}, with higher E_{eol} to the right of the flow direction (in the Northern Hemisphere).

Figures 6a–d show the variation of E_{eol} during the initial and intense stages of TC 04B (left panel) and TC 05B (right panel). The sea level height varied within a range of 8–10 dyn.cm from 1.2 to 2.0 m^2/s^2 on 15 October, and from 1.2 to 2.2 m^2/s^2 on 17 October (Figs. 6a–b). During the TC 05B, the sea-level height varied over a range of 20 dyn.cm from 0.6 to 2.6 m^2/s^2 on 25 October and a reduced range of 14 dyn.cm (0.6 and 2.0 m^2/s^2) during subsequent days (Figs. 6c–d). The inferred surface circulation is cyclonic (anticlockwise) around the center of the cyclone and anticyclonic (clockwise) at the rear end of the cyclone. On 15 October, the surface circulation was cyclonic north of 14 °N in the northwestern Bay and anticyclonic in the central Bay between 12 ° and 16 °N (Fig. 6a). The cyclonic circulation cell appeared to be coupled to the cyclonic vorticity zone associated with the winds around the center of cyclone (Fig. 2a). This is consistent with the dynamics associated with the response

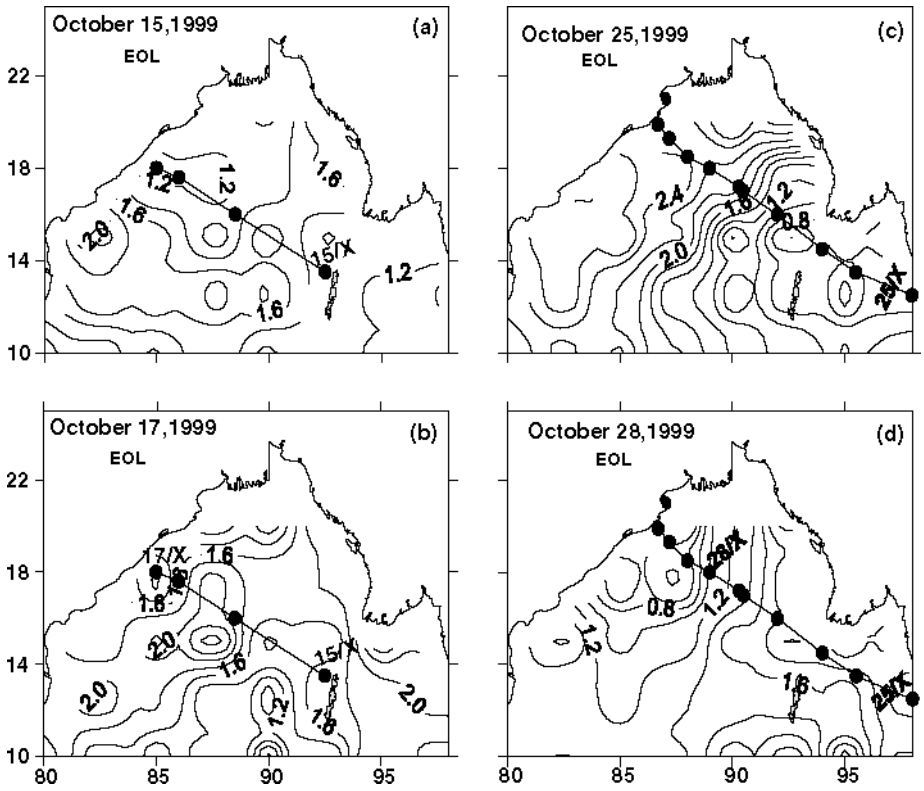

Figure 6
Variation of Effective Oceanic Layer (EOL) during various stages (initial and intense) of (a–b) TC 04B (left panel) and (c–d) TC 05B (right panel).

of the ocean to the wind field (p. 327; GILL, 1982). This coupling leads to the important observation of the presence of the surface Ekman divergence underneath the cyclone center (SHAY *et al.*, 2000) and geostrophic convergence at the outer edge of the cyclone.

As TC 05B intensified and moved across the Bay, the surface divergence zone also moved with it (Fig. 6b). The north/northwestward gradient in the estimated sea-surface height computed from the variation of E_{eol} during the period of cyclones resembles (qualitatively) that of the mean sea-level pressure, once again showing the response of ocean surface to the atmospheric forcing. The inferred surface eastward flow on 15 October (Fig. 6a) and southwestward flow on 17 October (Fig. 6b) in the central Bay agree with the measured currents at 3 m below the surface (qualitatively) at a moored buoy located at 13 °N, 87 °E as reported by CHINTHALU *et al.* (2001). On 25 October, the inferred surface circulation was cyclonic with its center (lower sea level) in the northern Andaman Sea and a south/southwesterly flow in the central Bay along the westward flank of the storm (Fig. 6c). Currents measured at 3 m below the sea surface by the moored data buoy at 13 °N, 87 °E confirm the inferred south/southwesterly flow in the central Bay (CHINTALU *et al.*, 2001). The cyclonic cell shifted northwestward as the weather system moved across the Bay and reached the northwestern Bay by 29 October. On the rear flank end of the system the surface circulation was anticyclonic. On 28 October the surface flow became northeasterly in the central Bay, opposite that seen on 25 October (Fig. 6d), which may be related to the inertial currents generated by the cyclone forcing. This identifies the quick response/change the surface flow adjusts/undergoes with the cyclonic wind forcing.

In the Arabian Sea, the 16 year-mean OLR and climatological EOL are negatively correlated in the month of May (EOL = −0.00072*OLR + 3.413 and r^2 = 0.9; MURTY *et al.*, 2004). Using this relation, the EOL was estimated (E_{eol}) from the daily OLR. During TC 01A the zone of intense convection (low OLR, 140–200 W/m^2), located to the left of the cyclone track (Figs. 5a–c), was characterized with higher E_{eol} (Figs. 7a–c). The inferred surface circulation associated with E_{eol} pattern is anticyclonic and the center of the weather system lay over the eastward flank of this anticyclonic cell. As the cyclone moved northward by 28 May, the intense convection zone also moved far northward. At the southeastern sector of the system a region of relatively higher OLR and lower EOL occurs, leading to cyclonic surface flow (Fig. 7c) and cooling at sea surface and deepening of MLD (see Sections 3.5.1 and 3.5.3).

3.4 Upper Ocean Response in the Bay of Bengal to the Tropical Cyclones

SHAY (1994) elaborated the thermal response and the momentum response, within the near-inertial dynamics, to the tropical cyclones on the upper ocean. RAO (2002) points out that there are two stages in the upper ocean response to the passage of cyclones; (1) local response which is mainly due to wind stress of the cyclone and

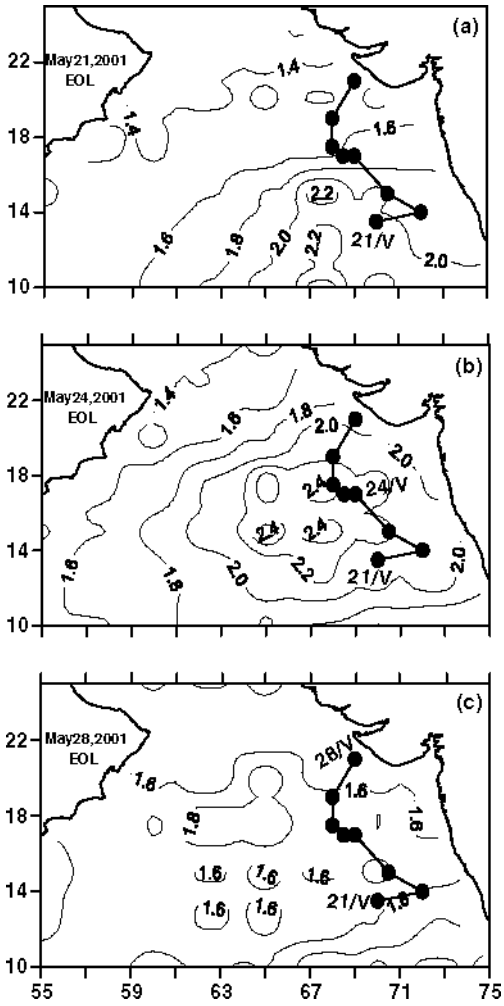

Figure 7
Variation of the Effective Oceanic Layer (EOL) during various stages (initial, intense and weakening) of TC 01A.

includes substantial cooling of SST and mixed layer and strong currents in the mixed layer (baroclinc) and geostrophic currents associated with the trough in sea-surface height (barotropic) and (2) nonlocal baroclinic response due to the wind-stress curl. In Section 3.3, the barotropic response of the upper ocean (top 30 m layer) was interpreted as a change in the surface circulation during the cyclone periods. In this section, the local-baroclinic response due to the cyclones on the SST, SSS and mixed layer depth will be examined.

The thermal response (SST variation) to the cyclones was obtained in three ways — first by estimating the SST from the algorithm ($E_{sst} = 0.718*E_{eol} + 27.26$ wherein

E_{eol} is the estimated EOL; $r^2 = 0.34$) for October; second by using the TRMM measured SST; and third by the NLOM simulated SST. The buoyancy response (SSS variation) to the cyclones is examined by comparing the estimated SSS (E_{sss}) from OLR with the MODAS SSS during the cyclone period. The variation of MLD during the cyclones is obtained from the NLOM simulations.

3.4.1 Sea Surface Temperature

When the weather system 04B formed as a 'Low pressure' on 14 October, the estimated SST (E_{sst}) showed a variation of ~1.4 °C between 27.8 °C and 29.2 °C with SST increasing towards the northwestern Bay and a cell of low SST (27.8 °C) north of Andaman Islands (not shown). When the 'Low pressure' area developed into a 'Depression' on 15 October, the range of SST sharply reduced to ~0.6 °C between 28.2 ° and 28.8 °C, with relatively cold waters (~28.2 °C) on to the right of the cyclone center (identifying the rightward bias) and warm waters (> 28.4 °C) to its left (Fig. 8a). As the weather system further developed into a 'cyclonic storm' and moved northwestward on 16 October, SST decreased to 27.6 °C in the northwestern Bay (ahead of the system). Between 15 and 16 October, the SST was 0.6 °C lower within the cyclone center in the northwestern Bay (18 °N, 85 °E). As the weather system intensified into VSCS on 17 October (Fig. 8b), the northwestern Bay experienced persistent cooling and the central Bay experienced warming of ~0.4 °C (from 28.4 °C on 16 October to 28.8 °C on 17 October) as the sky became cloud free. As the VSCS weather system weakened into a 'Deep Depression' and moved further north, an increase in SST was noticed on 20 October (figure not shown) ranging from 28.8 °C to 29.0 °C, which was identical to conditions that prevailed before the formation of the weather disturbance on 14 October. This suggests that it took about 7 days for revival of SST to return to ''normal'' conditions after the weather system preduced its effect on the Bay. GOPALAKRISHNA *et al.* (1993) reported a 2-week return period for the SST to reach normal conditions after a severe cyclone storm passed.

At the 'Depression' stage of TC 05B, the daily variation in the E_{sst} revealed a range of 1.6 °C with the occurrence of low SST (27.6 °C) beneath the cyclone center and warmer SST (28.8 °C) on the left and ahead of the storm (Fig. 8c). As the weather system moved northwestward, the region of cooler SST, coupled to the cyclone center, moved along with it while warmer SSTs occurred behind it (Fig. 8d). Therefore the direction of the SST gradient reversed, compared to that on 25 October (Fig. 8c). Surface cooling beneath the cyclone center and warming on its rear end are the noteworthy features. Though the weather system intensified further into a 'Super Cyclone' over land, its impact on the E_{sst} was not strong.

CHINTHALU *et al.* (2001), from the analysis of moored buoy data collected 3 m below the surface at 13 °N, 87 °E, reported a decrease in SST on the order of 0.7 °–0.9 °C as a response to the TC 04B and 05B. This measured SST was closer to the computed E_{sst} at the same location. This supports the finding that the

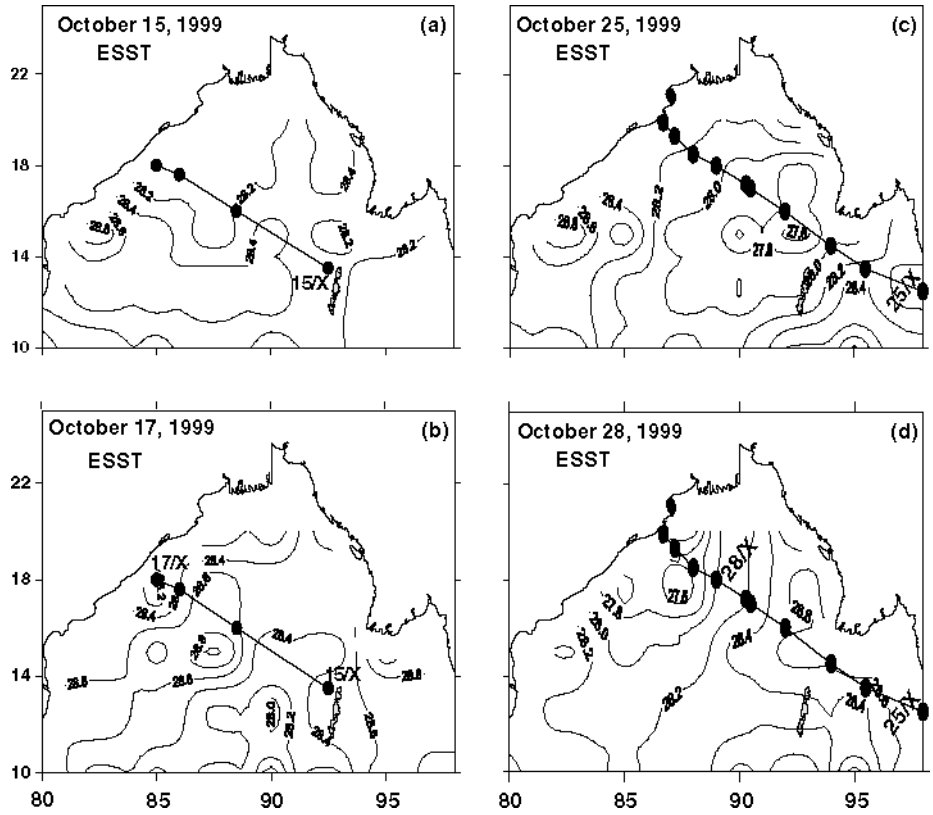

Figure 8
Variation of the estimated Sea Surface Temperature (E_{sst}) using the relationships between OLR, EOL and climatological SST during various stages (initial and intense) of (a-b) TC 04B (left panel) and (c-d) TC 05B (right panel).

estimation of SST using the daily OLR data through OLR-EOL-SST relationships could be a useful parameter to understand the thermal response processes and the prediction of the path of cyclones. Consideration of winds would improve the SST estimates.

The E_{sst} was also compared with TRMM SST (Figs. 9a–d) and NLOM SST (Figs. 10a–d) during the TC 04B and TC 05B. The TRMM SST was relatively higher compared to E_{sst}, with the TRMM SST on 17 October (weather system VSCS stage) warmer by 1.3 °C beneath the cyclone center and by 0.2 °–0.4 °C to the right of the cyclone center. Cooling in TRMM SST can also be seen along the tracks of TC 04 and TC 05B (Figs. 9b,d). While the variation of E_{sst} was ~0.6 °C, it was ~1.0 °C in TRMM SST and ~2.0 °C in NLOM SST along the cyclone track on 17 October (also on all the other days). On 28 October, the range of E_{sst} was 1 °C (27.6 °–28.6 °C) while the range of TRMM SST was as high as 2.0 °C (27.5 °–29.5 °C) and

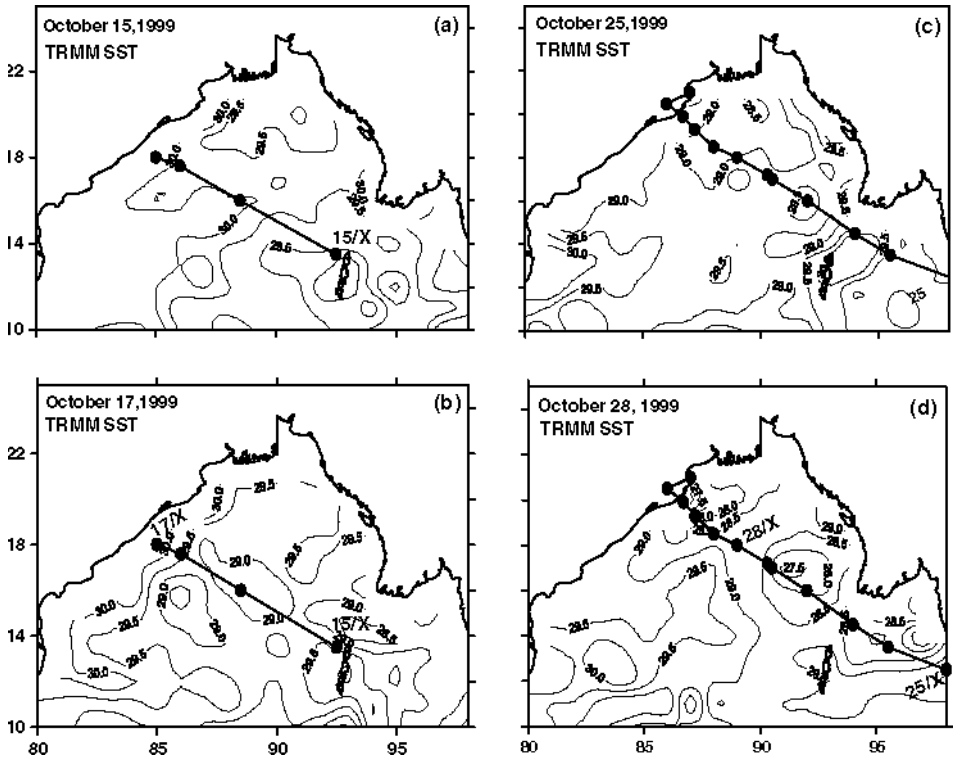

Figure 9
Variation of satellite measured TRMM SST during various stages (initial and intense) of (a–b) TC 04B (left panel) and (c–d) TC 05B (right panel).

the range of NLOM SST was 1 °C (27.5 °–28.5 °). The E_{sst} and the NLOM SST differed by 0.5 °C with cooling beneath the cyclone center and warming ahead of the cyclone center (Figs. 10a-d). The NLOM SST was always high in the direction of cyclone track (Figs. 10a-d), though it exhibited cooling beneath the cyclone center. The cooling of SST beneath the cyclone center arises from the upwelling due to the divergence of currents in the Ekman layer. It appears that the thermal response in SST cooling is evident in all the three types of SST variations.

3.4.2 Sea Surface Salinity

The estimated sea-surface salinity (E_{sss}) was computed from daily OLR using the 2nd degree polynomial relationship, $E_{sss} = -192.56 + 2.229*OLR - 0.0055*OLR*OLR$ and $r^2 = 0.41$. As well, we have limited the minimum estimated SSS to be 16.0. We find that the estimated SSS values from the 2nd degree polynomial are relatively better than those obtained from the linear relationship between OLR and SSS for the lower values of OLR associated with the tropical cyclones. The distribution of E_{sss}

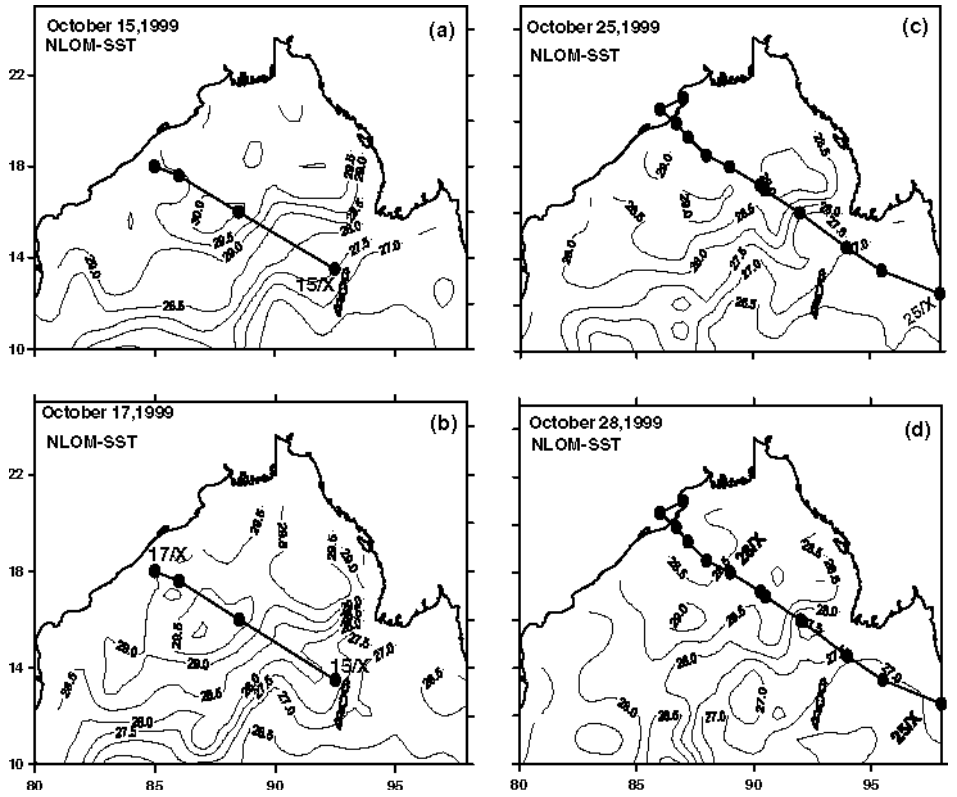

Figure 10
Variation of NLOM model simulated SST during various stages (initial and intense) of (a–b) TC 04B (left panel) and (c–d) TC 05B (right panel).

during the cyclone periods is presented in Figs. 11a–d. At first glance, it appears that the E_{sss} was far lower than the WOA98 SSS for the month of October. However, the variation of E_{sss} followed the TRMM rainfall pattern (not shown here), suggesting some part of the E_{sss} comes as a direct response to the precipitation associated with the cyclones. One would see cells of low salinity (as low as 18–20) beneath the cyclone center and along the track of the cyclone. The day-to-day variation of E_{sss} indicated that the cells of low salinity could be used for predicting the track of the cyclones from remote sensing measurements.

3.4.3 Mixed Layer Depth

The NLOM mixed layer depth was initially shallow (15 m) off the western Andaman Islands where the weather system was at 'depression' stage on 15 October (Figs. 12a–d). However, the MLD was deep (~30 m) ahead (in the direction of) of the cyclone and also on the left side of its track, at the region of maximum winds and

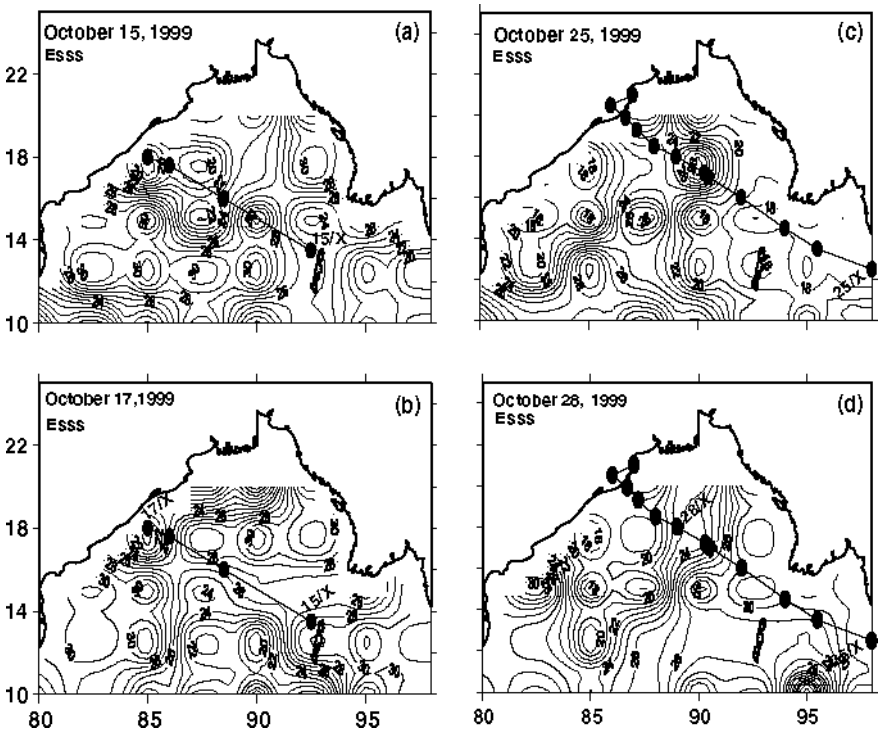

Figure 11
Variation of estimated Sea Surface Salinity (E_{sss}) using the relationship between OLR and climatological SSS during various stages (initial and intense) of TC 04B and 05B.

geostrophic convergence. This trend continued on subsequent days with shallow MLD developing near the Indian coast and a deepening of MLD to 55 m to the left side of the cyclone track between 14 ° and 16 °N. The cyclone 05B also moved over a region of shallow MLD (Figs. 12c-d) with deepening of the MLD to the left of the track. The trend of MLD variation is similar to that observed as in the case of TC 04B. The warm, deep mixed layer ahead of the cyclone provides necessary heat energy for the intensification of the cyclone. As the cyclone center passes over this deep mixed layer, the extraction of heat (due to turbulent air-sea heat fluxes) cools the mixed layer temperature and thus the SST. However, the occurrence of precipitation associated with the cyclone and the presence of low-salinity surface waters (Figs. 11a–d) lead to strong stratification and help maintain warmer SSTs (though cooled to a smaller extent by the cyclone) above 28.0 °C for the sustenance of the cyclones. The salinity stratification and shallow MLD are in turn responsible for the weaker response of SST (observed and estimated as in this study) to the intense cyclones (such as 04B and 05B) as reported through observations (MURTY *et al.*, 1996; SEETARAMAYYA *et al.*, 2001; CHINTHALU *et al.*, 2001). The cyclone-

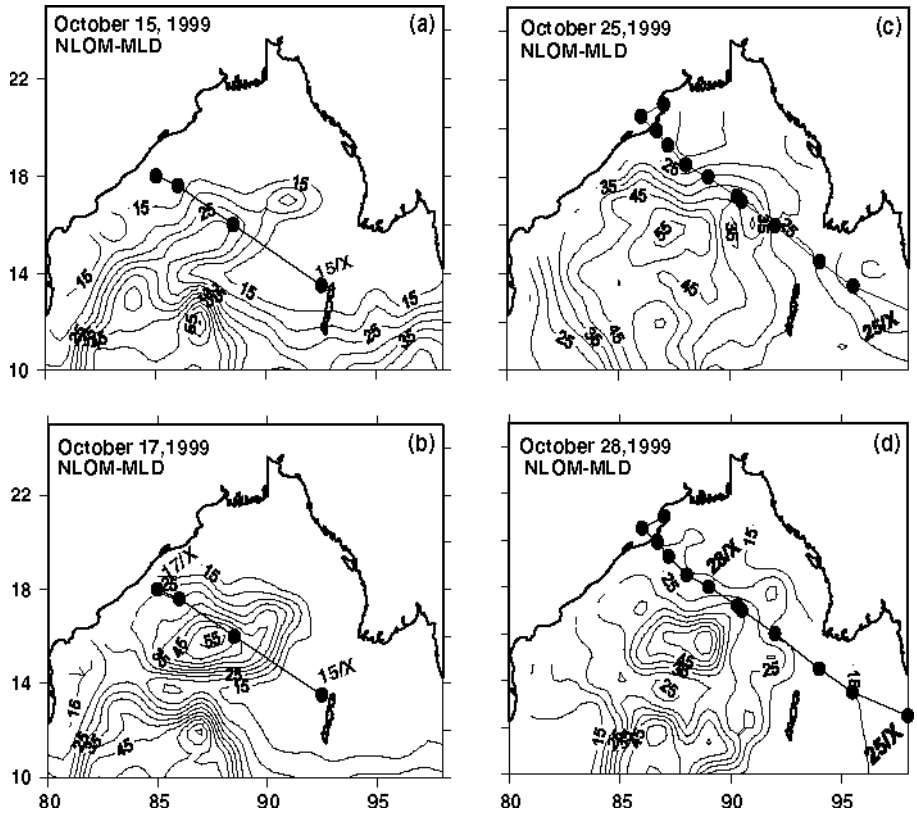

Figure 12
Variation of NLOM model simulated Mixed Layer Depth (MLD, m) during various stages (initial and intense) of (a–b) TC 04B (left panel) and (c–d) TC 05B (right panel).

induced divergence and the stratification lead to the development of a shallow mixed layer at the center of the cyclone with relatively moderate cooling (0.5–0.9 °C) limited to the stratified layer (i.e., mixed layer). This cooling process does not support further deepening of the mixed layer due to strong salinity stratification.

The isolines of MLD are closed across the track of the cyclone with larger MLD to the left of the track. Further, it is seen that the shallow MLD coincides with the lower E_{eol} beneath the cyclone center and the deep MLD with higher E_{eol} to the left side of cyclone track. The OLR shows intense convection ahead of the cyclone and relatively weakened convection to the left of the track. This has caused the estimated SST (using OLR-EOL-SST relationships) and TRMM SST to cool beneath the cyclone center and warm to the left of the cyclone track. When the weather system intensified, lower EOL was observed beneath the center of the cyclone and high on its periphery. These suggest that the cyclone-induced divergence (at the cyclone center) and convergence (at the maximum wind belt) are responsible for the variation of

simulated MLD and the associated response in sea-surface conditions (E_{eol}, E_{sst} and E_{sss}, the parameters derived from the OLR).

Thus, it appears that the coupling between the OLR and EOL (through variation in sea-level height, inferred surface circulation, estimated SST and SSS) is useful to predict the path of tropical cyclones or even the monsoon depressions. GOSWAMI (1987) showed that the moisture convergence (or precipitation) on the western sector of a cyclone is responsible for the observed west-northwestward movement of the monsoon depressions that form during the southwest monsoon (June–September) in the northern Bay.

3.5 Upper Ocean Response in the Arabian Sea to the Tropical Cyclone 01A

3.5.1 Sea Surface Temperature

In the Arabian Sea, the estimated SST [$E_{sst} = 2.3055*E_{eol} + 25.8984$ and $r^2 = 0.56$, where the E_{eol} is the estimated EOL] during the period of cyclone is presented in Figs. 13a–c. The day-to-day change of E_{sst} is examined from 21 May to 28 May (shown here only for May 21, 24 and 28, 2001). The superposition of cyclone track on the daily E_{sst} maps indicates that the weather disturbance formed over the warmer SST (30.5–31.0 °C) region in the southeastern Arabian Sea. The extent of warmer waters (> 30.0 °C) on 21 May suggests the presence of Arabian Sea warm pool with core values of SST (31 °C) at 12 °N, 68 °E. The E_{sst} increases from 21 May to 24 May with a core value of 31.5 °C. This warmer SST prevails until 26 May and the position of the weather system is coupled to the warmer SST on these days. With the northward movement of the cyclone on 27 May, the SST cools by 1.5 °C east of 68 °E when compared to the E_{sst} on 24 May and cools by ~0.5 °C from E_{sst} on 26 May. The TRMM SST (Figs. 14 a–c) is closer to the E_{sst}. The TRMM SST effects cooling from 23 May onwards with intense cooling beneath the cyclone center and in the area behind the cyclone. The NLOM SST (Figs. 14d-f) shows warmer SSTs (29 °–30 °C) in the southeastern Arabian Sea from 21 May to 25 May. By 26 May, the NLOM SST exhibits a thermal response to the cyclone and is cooled by 0.5 °C in the area traversed by the cyclone. On 28 May, TRMM SST shows an artifact of abnormal cooling of 5 °C due to heavy precipitation and masks the cooling due to the cyclone. The cell of low SST coincides with the cell of heavy precipitation obtained from TRMM rainfall measurements (figure not shown).

3.5.2 Variation of Sea Surface Salinity

The estimated SSS (E_{sss}) during the cyclone period is obtained using the linear relationship, $E_{sss} = 0.024*OLR + 29.712$; $r^2 = 0.89$ (MURTY *et al.*, 2004) and is presented in Figs. 15a–c. The observed salinity difference (unlike in the Bay of Bengal) was smaller at the center of the cyclone (where the OLR was the lowest). An examination of the E_{sss} indicates that the cyclonic system formed and intensified over the region of low SSS. The minimum E_{sss} of 33.0 was observed on

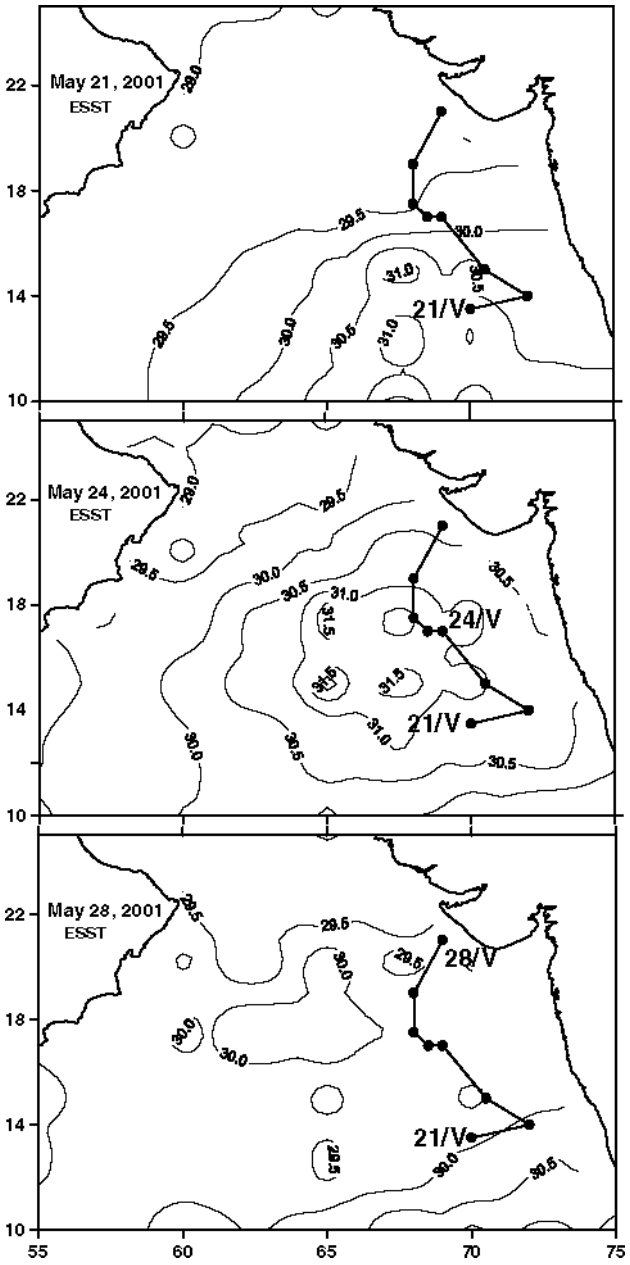

Figure 13
Variation of (a–c) estimated Sea Surface Temperature (E_{sst}) using the relationships between OLR, EOL and climatological SST during various stages (initial, intense and weakening) of TC 01A.

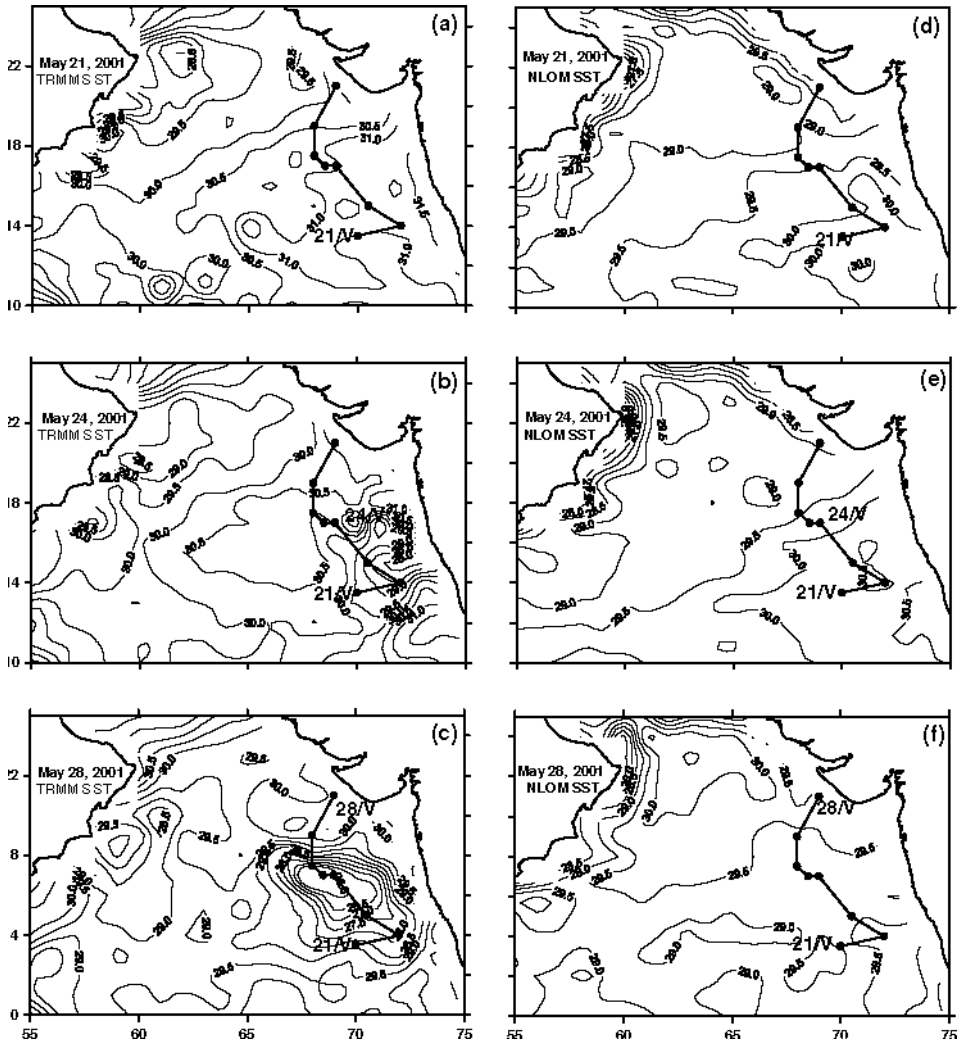

Figure 14
Variation of (a–c) satellite measured TRMM SST and (d–f) NLOM model simulated SST during various stages (initial, intense and weakening) of TC 01A.

23–24 May when the atmospheric system was fully developed (Fig. 15b). The weather system was nearly stationary at 17 °N, 68 °E from 24 May to 26 May. Subsequently, the weather system moved northward on 27 May over the region of relatively higher E_{sss} and weakened as it moved towards the Indian coast (Fig. 15c). In the southeastern Arabian Sea, the E_{sss} increased when the cyclone moved farther north coinciding with the lower SSTs. It is noted that the center of the cyclone is coupled to the warmer and low saline waters.

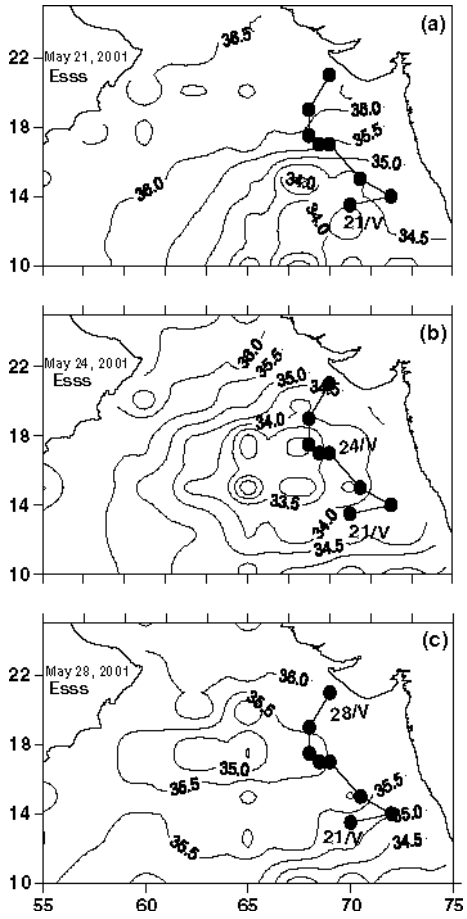

Figure 15
Variation of estimated Sea Surface Salinity (E_{sss}) using the relationship between OLR and climatological SSS during various stages (initial, intense and weakening) of TC 01A.

3.5.3 Variation of Upper Ocean Mixed Layer Depth

The inferred surface circulation from EOL (Figs. 7a–c) correlates well with the NLOM MLD (Figs. 16a–c). In the geostrophic convergence region the MLD is deep, and at the center of the cyclone the MLD is shallow. Moreover, as the cyclone moves northward, the MLD increases in the region behind the cyclone. As the estimated SST cools, the MLD deepens. This suggests that the OLR estimate of SST is realistic. Superposition of cyclone track on the daily NLOM MLD maps shows that the cyclone moves over the shallow MLD (~15 m) region. In accordance with the generally intense warming during May and the associated warmer SSTs from 21 May (Fig. 16a) to 23 May, the MLD was ~12 m in the cyclone-influenced area. As the cyclone intensified, a slight (~3 M) deepening in MLD was noticed on 24 May

(Fig. 16b), with further deepening up to 28 m between 25 May and 28 May (Fig. 16c). It is observed that the MLD variation is closely related to the E_{eol} variation. This means that the geostrophic near-surface flow associated with the EOL governs the MLD distribution. The isolines of MLD run west-east with larger MLD on the equatorward side. This suggests that the MLD deepening is more biased to the left of the cyclone track and is due to the convergence of geostrophic flow at the periphery of the cyclone (SUBRAHMANYAM *et al.*, 2002). The cooling of NLOM SST on 26 May and 27 May might be a result of entrainment followed by mixing and deepening of the MLD.

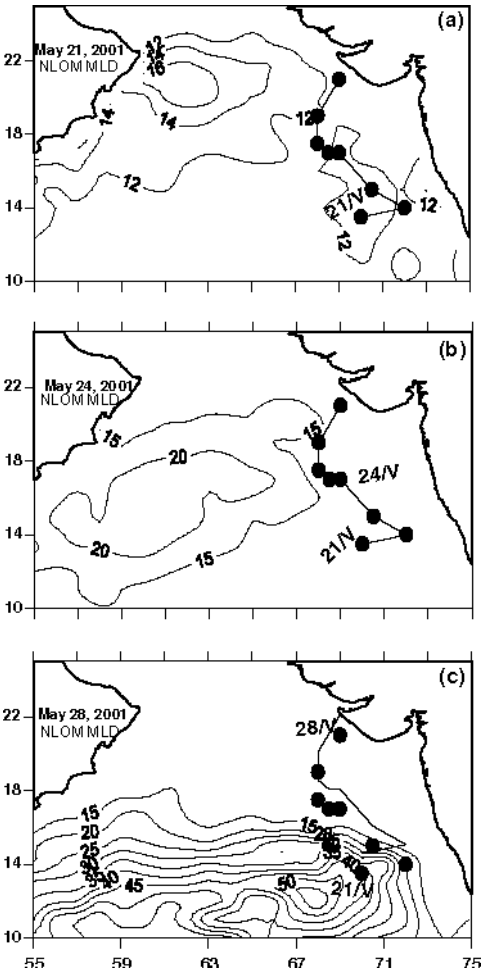

Figure 16
Variation of (a–c) NLOM model simulated Mixed Layer Depth (MLD, m) during various stages (initial, intense and weakening) of TC 01A.

3.6 Comparison of Estimated SST and SSS with the Time-series Observations during Synoptic Scale Conditions

In this study, dealing with the synoptic weather systems and the associated air-sea coupling, we have applied the algorithms that were derived using the climatological data sets (16 year-mean monthly OLR data, computed monthly EOL using WOA98 temperature and salinity data, and WOA98 SST and SSS data) for the Bay of Bengal and the Arabian Sea (MURTY *et al*., 2004). In order to assess the extent to which these algorithms suit the synoptic scale studies, we have made use of the short-term time-series temperature and salinity data collected at 3 hourly intervals in the northern Bay of Bengal at 17.5 °N, 89 °E during the Bay of Bengal Monsoon Experiment (BOBMEX) in 1999 (BHAT *et al*., 2001; VINAYACHANDRAN *et al*., 2003). The time-series data in the upper 30 m were daily averaged and used to compute the daily time-series of EOL. The INSAT 1-D satellite derived daily OLR data during the BOBMEX period (Phase I: 27 July-5 August, 1999) were used to estimate the SST and SSS using the algorithms (MURTY *et al*., 2004) for July and August. The SSS is also estimated using the climatological OLR-SSS relationships for July and August (MURTY *et al*., 2004). It is mentioned that Phase I of BOBMEX-99 period was characterized by intense convection with the occurrence of synoptic weather disturbances (BHAT *et al*., 2001). The daily OLR arising from the presence of weather disturbances was quite low, compared to the climatological OLR. Figures 17a–b display the comparison of the daily variation of estimated and observed SST and SSS during 27 July-5 August 1999. The values of both the SSTs are closer and their deviations (estimated minus observed SST) give rise to a mean value of –0.01 °C with a standard deviation (SD) of 0.33 °C. One would see that the SST patterns are opposite, as we have not considered other factors such as winds and advection. The estimated SSS values from both the algorithms of SSS, however, are higher than the observed SSS, partly due to nonconsideration of freshwater flux due to evaporation minus precipitation, horizontal advection and mixing in the mixed layer. However, the mean and SD values of SSS deviations are 1.83 ± 2.5 for the OLR-EOL-SSS algorithms and 1.95 ± 1.76 for the OLR-SSS algorithms. We feel that these statistical values are reasonable partly because only 10 days data were used for comparison and partly due to the application of the climatological data based algorithms to the synoptic situation.

4. Conclusions

This study addresses the thermal, salinity and circulation responses at sea surface due to intense tropical cyclones in 1999 and 2001 in the northern tropical Indian Ocean, based on satellite measurements and model simulations, to understand the

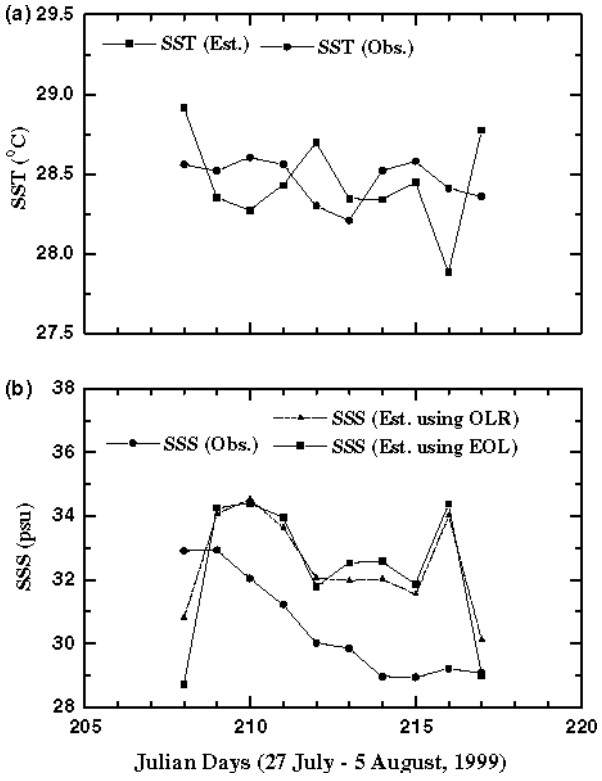

Figure 17
Daily variation of (a) observed SST (dots) and estimated SST (squares) from OLR-EOL-SST algorithms and (b) observed SSS (dots) and estimated SSS from OLR-EOL-SSS algorithms (squares) and from OLR-SSS algorithms (triangles) in the northern Bay of Bengal (17.5°N, 89°E) during 27 July – 5 August, 1999.

air-sea coupling processes. In this study, it is shown that through the relationships between the OLR and EOL, one can estimate the SST, SSS and sea surface elevation which are closely coupled to the oceanic mixed layer depth. It is envisaged that this coupling advances prediction of the path of weather systems in the northern Indian Ocean. The thermal response to the cyclones is documented from the OLR derived SST with the magnitudes of SST cooling falling within the range of reported values. The SST cooling occurred beneath the cyclone center in the Bay of Bengal. However, in the Arabian Sea the SST cooling occurred only a few days after the cyclone had passed over the area. This difference in the air-sea coupling processes is mainly a result of the difference in upper-ocean stratification (related to the EOL parameter); specifically saline stratification in the Bay of Bengal and thermal stratification in the Arabian Sea and the associated mixing processes.

In this study, the salinity response to the cyclones is attempted in terms of estimated SSS variation. In this direction, it is shown that nearly realistic

information regarding the daily SSS pattern can be obtained in the vicinity and along the track of cyclones from satellite observations of OLR and would prove helpful until space-borne satellite measurements of salinity are available. The occurrence of cells of low SSS (estimated) beneath the cyclone center (in the Bay of Bengal) suggests intense precipitation associated with the cyclones. Comparison of the OLR derived salinity product with the US Navy's MODAS SSS, both in the Bay of Bengal on 28 October, 1999 and in the Arabian Sea on 24 May 2001, is presented in Figs. 18a–c. The daily MODAS SSS is closer to the monthly WOA98 SSS (Figs. 18b–d), suggesting that the MODAS SSS is good only for longer time scales (weeks or months) and does not depict the surface salinity (SSS) response due to synoptic weather systems.

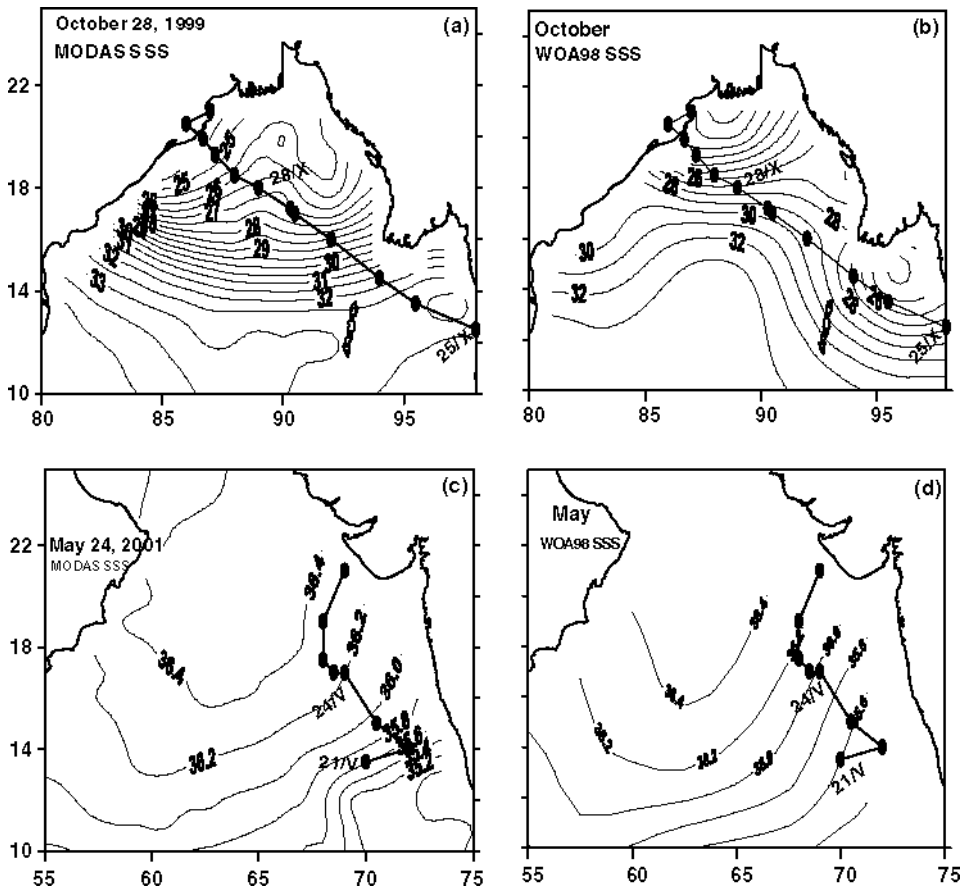

Figure 18
Variation of (a) MODAS SSS and (b) WOA98 SSS in the Bay of Bengal (top panel), (c) MODAS SSS and (d) WOA98 SSS in the Arabian Sea (bottom panel).

Acknowledgements

The interpolated OLR data is provided by the NOAA-CIRES CDC. We thank Dr. Harley Hurlburt and Dr. Birol Kara for providing the NLOM MLD simulations and Dr. Charlie Barron for providing the MODAS sea-surface salinity data. Dr. Mark Bourassa made available the QuikSCAT Scatterometer data on COAPS/FSU web page. TRMM TMI data and images are produced by Remote Sensing Systems and sponsored by NASA's Earth Science Information Partnerships (ESIP): a federation of information sites for Earth Science; and by NASA's TRMM Science Team. Bulusu Subrahmanyam is supported by NASA/JPL grant #961434. The COAPS at the FSU receives its base support from the NASA Physical Oceanography Program and through the Applied Research Center, funded by NOAA Office of Global Programs and also from ONR's Secretary of the Navy Grant awarded to Dr. James J. O'Brien. The BOBMEX programme was supported by the Department of Science and Technology, New Delhi. Dr. V.S.N. MURTY thanks Dr. S.R. Shetye, Director, NIO, India, for his keen interest in this study and also DST, India for funding BOBMEX project. NIO contribution No. 3893.

REFERENCES

ANONYMOUS, (1979), *Tracks of Storms and Depressions in the Bay of Bengal and the Arabian Sea 1877–1970,* India Meteorological Department, New Delhi, Charts 1–186.

ANTONOV, J., LEVIUTS, S., BOYER, T.P., CONKRIGHT, M., O'BREIN, T., STEPHENS, C., and TROTSENKO, B. (1998), *World Ocean Atlas 1998, vol. 3: Temperature of the Indian Ocean,* NOAA Atlas NESDIS 29. U.S. Gov. Printing Office, Washington, D.C., pp. 1–166.

BHAT, G.S., GADGIL, S., HARISH KUMAR, P.V., KALSI, S.R., MADHUSOODANAN, P., MURTY, V.S.N., PRASADA RAO, C.V.K., RAMESH BABU, V., RAO, L.V.G., RAVICHANDRAN, M., REDDY, K.G., SANJEEVA RAO, P., SENGUPTA, D., SIKKA, D.R., SWAIN, J., and VINAYACHANDRAN, P. (2001), *BOBMEX — the Bay of Bengal Monsoon Experiment*, Bull. Amer. Meteor. Soc. *82*, 2217–2243.

BOYER, T.P., LEVIUTS, S., ANTONOV, J., CONKRIGHT, M., O'BRIEN, T., STEPHENS, C., and TROTSENKO, B. (1998), *World Ocean Atlas 1998, vol. 6: Salinity of the Indian Ocean,* NOAA Atlas NESDIS 32. U.S. Gov. Printing Office, Washington, D.C., pp. 1–166.

CHINTHALU, G.R., SEETARAMAYYA, P., RAVINDRAN, M., and MAHAJAN, P.N. (2001), *Response of the Bay of Bengal to Gopalpur and Paradip Super Cyclones during 15–31 October, 1999*, Curr. Sci. *81* (5), 283–291.

FOX, D.N., TEAGUE, W.J., BARRON, C.N., CARNES, M.R., and. LEE, C.M. (2002a), *The Modular Ocean Data Analysis System (MODAS)*, J. Atmos. Oceanic Technol. *19*, 240–252.

FOX, D.N., BARRON, C.N., CARNES, M.R., BOODA, M., PEGGION, G., and GURLEY, J.V. (2002b), *The Modular Ocean Data Analysis System*, Oceanography *15*, 22–28.

GILL, A.E., Atmosphere-Ocean Dynamics. *International Geophysical Series 30* (Academic Press 1982) pp. 1–662.

GINIS, I. (2002), Hurricane-ocean interactions, 2002. Tropical cyclone-ocean interactions. Chapter 3. In *Atmosphere – Ocean Interactions* (ed. Perrie, W.) (WIT Press 2002) *Advances in Fluid Mechanics Series*, pp. 33, 83–114.

GOPALAKRISHNA, V.V., MURTY, V.S.N., SARMA, M.S.S., and SASTRY, J.S. (1993), *Thermal Response of Upper Layers of Bay of Bengal to Forcing of a Severe Cyclonic Storm: A Case Study*, Indian J. Mar. Sci. 22, 8–11.

GOSWAMI, B.N. (1987), *A Mechanism for the West-north-west Movement of Monsoon Depressions*, Nature, *326*, 376–378.

HILBURN, K.A., BOURASSA, M.A., and O'BRIEN, J.J. (2003), *Scatterometer-derived Research-Quality Surface Pressure Fields for the Southern Ocean*, J. Geophys. Res. *108*, doi: 10.1029/2003JC001772, 37–1 to 37–11.

KARA, A.B., ROCHFORD, P.A., and HURLBURT, H.E. (2000), *An Optimal Definition for Ocean Mixed Layer Depth*, J. Geophys. Res. *105*, 16,803–16,821.

KARA, A.B., ROCHFORD, P.A., and HURLBURT, H.E. (2003a), *Mixed Layer Depth Variability Over the Global Ocean*, J. Geophys. Res. *108*, doi:10.1029/2000JC000736, 24–1 to 24–15.

KARA, A.B., WALLCRAFT, A.J. and HURLBURT, H.E. (2003b), *Climatological SST and MLD Predictions from a Global Layered Ocean Model with an Embedded Mixed Layer*, J. Atmos. Oceanic Technol, *20*, 1616–1632.

LAL, M. (2001), *Tropical Cyclones in a Warmer World*, Current Science *80*, 1103–1104.

LEVITUS, S. and BOYER, T.P. (1994a), *World Ocean Atlas 1994, vol. 4, Temperature*, NOAA Atlas, NESDIS, vol. 4, U.S. Department of Commerce, Washington D.C., U.S.A. pp. 1–117.

LEVITUS, S., BURGETT, R., and BOYER, T.P. (1994b), *World Ocean Atlas 1994, vol. 3, Salinity*, NOAA Atlas, NESDIS, vol. 4, U.S. Department of Commerce, Washington D.C., USA, pp 1–99.

MURTY, V.S.N. (1983), The lowering of sea-surface temperature in the east central Arabian Sea associated with a cyclone, Mahasagar — Bull. Natl. Inst.Oceanogr*, 16*, 67–71.

MURTY, V.S.N., SARMA, Y.V.B., and RAO, D.P. (1996), *Variability of the Oceanic Boundary Layer Characteristics in the Northern Bay of Bengal during MONTBLEX-90*, Proc. Indian Acad. Sci. (Earth Planet. Sci.), *105*, 41–61.

MURTY, V.S.N., SARMA, M.S.S., TILVI, V. (2000), Seasonal cyclogenesis and the role of the near-surface stratified layer in the Bay of Bengal. In *PORSEC Proceedings*, Vol. I, NIO, Goa, India during 5–8 December, 2000, pp. 453–457.

MURTY, V.S.N., SUBRAHMANYAM, B., SARMA, M.S.S., TILVI, V., and RAMESH BABU, V. (2002), *Estimation of Sea Surface Salinity in the Bay of Bengal using Outgoing Longwave Radiation,* Geophys. Res. Lett. *29*, doi: 10.1029/2001GL014424, 11–1 to 11–4.

MURTY, V.S.N., SUBRAHMANYAM, B., TILVI, V., and O'BRIEN, J.J. (2004), *A new technique for the estimation of sea surface salinity in the tropical Indian ocean from OLR*, J. Geophys. Res., 109, C12006, doi: 10.1029/2003JC001928.

OBASI, G.O.P. (1997), *WMO's Programme on Tropical Cyclone*, Mausam, *48*, 103–112.

PREMKUMAR, K., RAVICHANDRAN, M., KALSI, S.R., SENGUPTA, D., and GADGIL, S. (2000), *First Results from a New Observational System over the Indian Seas,* Curr. Sci. *78*(3), 323–330.

RAO, R.R. (1987), *Further Analysis on the Thermal Response of the Upper Bay of Bengal to the Forcing of Pre-monsoon Cyclonic Storm and Summer Monsoonal Onset during MONEX-79*, Mausam *38*, 147–156.

RAO, Y.R. (2002), *The Bay of Bengal and Tropical Cyclones*, Curr. Sci. *82*, 379–381.

SHARP, R.J. BOURASSA, M.A., and O'BRIEN, J.J. (2002), *Early Detection of Tropical Cyclones Using SeaWinds Derived Vorticity*, Bull. Am. Meteor. Soc. *83*, 879–889.

SHAY, L.K., Oceanic response to tropical cyclones. In *The Oceans: Physical-Chemical Dynamics and Human Impact* (eds. S.K. Mujumdar, E.W. Miller, G.S. Forbes, R.F. Schmalz, and Assad A. Panah) (The Pennsylvania Academy of Science 1994) pp. 1–497.

SHAY, L., GONI, G.J., and BLACK, P.G. (2000), Effects of Warm Oceanic Feature on Hurricane Opal, Mon. Weath. Rev., *128*, 1367–1383.

SEETARAMAYYA, P., NAGAR, S.G., and MULLAN, A.H. (2001), *Response of the North Bay of Bengal (Head Bay) to Monsoon Depression during MONTBLEX-90*, The Global Atmos. and Ocean Sys. *7*, 325–345.

STRAMMA, L., CORNILLON, P., and PRICE, J.F. (1986), *Satellite Observations of Sea-surface Cooling by Hurricanes*, J. Geophys. Res. *91*, 5031–5035.

SUBRAHMANYAM, B., RAO, K.H., SRINIVASA RAO, N., MURTY, V.S.N., and SHARP, R.J. (2002), *Influence of a Tropical Cyclone on Chlorophyll-1 Concentration in the Arabian Sea*, Geophys. Res. Lett. *29*, doi:10.1029/2002GL015892, 22–1 to 22–4.

TURK, G. and BANKS, D.C. (1996), *Image-Guided Streamline Placement*, Computer Graphics, SIGGRAPH 96 Conf. Proceedings, pp. 453–460.

VINAYCHANDRAN, P.N., MURTY, V.S.N., and RAMESH BABU, V. (2002), *Observations of Barrier Layer Formation in the Bay of Bengal during Southwest Monsoon*, J. Geophys. Res. *107*, 8018, doi:10.1029/2001JC000831. SRF 19-1 to SRF 19-9.

(Received October 14, 2003; accepted April 29, 2004)